Female and Male Gamete Mitochondria Are Distinct and Complementary in Transcription, Structure, and Genome Function

Wilson B.M. de Paula[1], Ahmed-Noor A. Agip[1,7], Fanis Missirlis[2], Rachel Ashworth[3], Gema Vizcay-Barrena[4], Cathy H. Lucas[5], and John F. Allen[1,6,*]

[1]School of Biological and Chemical Sciences, Queen Mary University of London, London, United Kingdom

[2]Departamento de Fisiología, Biofísica y Neurociencias, Centro de Investigación y de Estudios Avanzados del Instituto Politécnico Nacional, Del. Gustavo A. Madero, México

[3]School of Medicine and Dentistry, Queen Mary University of London, The Blizard Institute, London, United Kingdom

[4]Centre for Ultrastructural Imaging, King's College London, London, United Kingdom

[5]Ocean and Earth Science, National Oceanography Centre Southampton, University of Southampton, Southampton, United Kingdom

[6]Research Department of Genetics, Evolution, and Environment, University College London, London, United Kingdom

[7] Present address: MRC Mitochondrial Biology Unit, Wellcome Trust/MRC Building, Hills Road, Cambridge, United Kingdom

*Corresponding author: E-mail: j.f.allen@qmul.ac.uk.

Accepted: September 23, 2013

Abstract

Respiratory electron transport in mitochondria is coupled to ATP synthesis while generating mutagenic oxygen free radicals. Mitochondrial DNA mutation then accumulates with age, and may set a limit to the lifespan of individual, multicellular organisms. Why is this mutation not inherited? Here we demonstrate that female gametes—oocytes—have unusually small and simple mitochondria that are suppressed for DNA transcription, electron transport, and free radical production. By contrast, male gametes—sperm—and somatic cells of both sexes transcribe mitochondrial genes for respiratory electron carriers and produce oxygen free radicals. This germ-line division between mitochondria of sperm and egg is observed in both the vinegar fruitfly and the zebrafish—species spanning a major evolutionary divide within the animal kingdom. We interpret these findings as an evidence that oocyte mitochondria serve primarily as genetic templates, giving rise, irreversibly and in each new generation, to the familiar energy-transducing mitochondria of somatic cells and male gametes. Suppressed mitochondrial metabolism in the female germ line may therefore constitute a mechanism for increasing the fidelity of mitochondrial DNA inheritance.

Key words: mitochondrial DNA, maternal inheritance, *Drosophila melanogaster*, *Danio rerio*, reactive oxygen species, aging.

Introduction

Mitochondria are eukaryotic subcellular organelles with key roles in ATP synthesis, programmed cell death (Vaux et al. 1988), Fe-S cluster assembly (Lill and Kispal 2000), and aging (Harman 1972). Mitochondria originated as prokaryotic endosymbionts and still carry the remnant of an α-proteobacterial genome (Pesole et al. 2012)—in animals usually only 13 protein-coding genes (Anderson et al. 1981; Gray et al. 1999). These genes encode core subunits of the respiratory electron transport chain, which generates ATP by means of oxidative phosphorylation (Mitchell 1961). Three respiratory chain complexes contain both mitochondrial and nuclear gene products, the latter being imported, as precursors, after synthesis on cytosolic ribosomes. Mitochondrial DNA (mtDNA) is exposed to mutagenic reactive oxygen species (ROS) generated as a by-product electron transport in the inner mitochondrial membrane. ROS are produced initially by transfers of single electrons to O_2, to give the superoxide anion radical, and contribute to deleterious mtDNA rearrangements that result in severe diseases in humans (Ames et al. 1995; Balaban et al. 2005; Wallace 2010). These diseases include Pearson syndrome, Leigh syndrome, Leber hereditary myopathy, and some cardiomyopathies, with associated effects including renal failure, Alzheimer's disease, and Parkinson's disease

(Wallace 2007). mtDNA mutation is thought to occur either in the female germ line or early in embryonic development (Wallace et al. 1995), yet surprisingly, few mutations are transmitted to each successive generation. For this, two main theories are currently debated.

The mitochondrial genetic bottleneck theory states that, prior to oogenesis, the population of maternal mtDNA molecules in primordial germ cells decreases in size, causing a genetic bottleneck in which random drift segregates different mtDNAs (Samuels et al. 2010). Some cells, with decreased mitochondrial heteroplasmy, may then be selected as beneficial to the developing embryo (Samuels et al. 2010). However, studies conclude that no reduction of mtDNA copy number occurs in primordial germ cells (Cao et al. 2009), while other studies arrive at differing conclusions on variance of mtDNA between oocytes and developing embryos (Jenuth et al. 1996; Wai et al. 2008). The second theory, an addition to the bottleneck theory, is that of a "purifying sieve" in the female germ line; a filter that discriminates between "healthy" and "unhealthy" mitochondria, allowing only the former to populate the offspring. These proposals are supported by results showing the elimination of a severe mtDNA mutation after a number of generations (Fan et al. 2008), or by low nonsynonymous/synonymous substitution (d_N/d_S) ratios observed in mtDNA sequences over generations (Stewart et al. 2008).

A third and independent hypothesis for faithful transmission of mtDNA states that oocyte mitochondria are transcriptionally and energetically repressed and hence fail to generate mutagenic ROS at the same rate as mitochondria of sperm and somatic cells. According to this view, separation of a line of quiescent, template mitochondria maintains the integrity of mtDNA through the female germ line and between generations (Allen 1996; Allen and de Paula 2013). This hypothesis appears to be consistent with observations reported for mitochondria of a cnidarian, the jellyfish *Aurelia aurita* (de Paula et al. 2013). Here we report results of experiments designed to test whether specific suppression of oocyte mitochondrial function extends more widely within the animal kingdom. Accordingly, our experimental subjects were an insect, the fruitfly *Drosophila melanogaster,* and a vertebrate, the zebrafish *Danio rerio.* Insects and vertebrates are lineages of protostomes and deuterostomes, respectively, and any general conclusion might be taken to stand for the Bilateria as a whole.

Materials and Methods

Drosophila melanogaster strains were maintained on standard cornmeal/yeast/agar medium at 25 °C (Sadraie and Missirlis 2011). Wild-type flies had been collected from Tannes, Italy. Bloomington stock 7194 P{sqh-EYFP-Mito} carries a P-element insertion including the spaghetti squash (sqh) promoter driving expression of the enhanced yellow fluorescent protein (EYFP) tagged at the N-terminal end with a mitochondrial targeting sequence (LaJeunesse et al. 2004). *Danio rerio* wild-type strains (Tubingen and Tupfel long fin) were bred and raised in-house at the zebrafish facility of Queen Mary, University of London, UK, as previously described by Zimprich et al. (1998). Work on zebrafish was conducted in accordance with the UK Animals (Scientific Procedures) Act 1986, with prior approval by the local institutional animal care committee. Adult fish were euthanized using a lethal dose of anesthetic (Tricaine methanesulfonate, MS-222), and tissues were dissected immediately.

Total mRNA from dissected tissues was isolated using TRI Reagent (Ambion), treated with DNase I (New England Biolabs) for 10 min at 37 °C and repurified using Pure LinkTM RNA Mini Kit (Ambion), all according to the manufacturer instructions. Quantitative real-time polymerase chain reaction (qRT-PCR) was carried out using a Chromo4 real-time detector (Bio-Rad) and Brilliant III Ultra-Fast SYBR Green qRT-PCR (Agilent). All messenger RNA quantities were normalized against nuclear-encoded genes rpL32 for *D. melanogaster* and β-actin for *D. rerio*. A second normalization was done using intestine average values from both sexes as the calibration tissue. The primers used in this study are described in supplementary table S1, Supplementary Material online. Three technical replicates for each biological replicate were averaged at the beginning, and three biological replicates were used to generate the error bars. $C(t)$ values were analyzed using qBase PLUS2 software (Biogazelle). One-way analysis of variance (ANOVA) with post-Tukey's multiple comparison test with a significance level set at $P \leq 0.05$ was used as statistical treatment (supplementary table S2, Supplementary Material online).

Confocal light microscopy was employed to visualize and compare mitochondrial inner membrane potential and production of ROS. For mitochondrial membrane potential analysis, freshly dissected tissues were equilibrated in 500 nM Mitotracker Red FM (Molecular Probes) dissolved in phosphate buffered saline (PBS) for approximately 30 min at room temperature. For zebrafish only, an additional 500 nM of Mitotracker Green FM was used simultaneously. Three washes in pure PBS were used to remove the probe excess. For ROS detection, we followed the method described by Owusu-Ansah et al. (2008) with minor modifications. Freshly dissected tissues were equilibrated in a solution containing 2′,7′-dichlorodihydrofluorescein (H_2DCF-DA, Sigma) at 10 μM final concentration, also containing 4′,6-diamidino-2-phenylindole dihydrochloride (DAPI) (Sigma) at 1 μM final concentration, at room temperature PBS for 30 min, followed by three PBS washes. Microscopy was performed using a Leica TCS SP5 confocal microscope (Leica Microsystems). Excitation and emission wavelengths were selected for the different probes as follows: DAPI, 350 nm/450–480 nm; H_2DCF-DA, 488 nm/520–550 nm; Mitotracker Green, 488/500–530 nm; YFP, 514/520–560 nm; and Mitotracker Red, 581/620–650 nm. Imaging was performed with a 63× lens, and laser

output was kept under 15% of maximal power. Leica LAS AF software was used to acquire the images. ImageJ software (Schneider et al. 2012) was used to measure and calculate the mean pixel intensity of 8-bit acquired images (0–255).

For transmission electron microscopy (TEM), specimens were fixed overnight in 2.5% (v/v) glutaraldehyde in 0.1 M cacodylate buffer (pH 7.3) and postfixed in 1% (w/v) osmium tetroxide in 0.1 M cacodylate buffer (pH 7.3) for 1.5 h. Samples were then dehydrated through a graded ethanol series, equilibrated with propylene oxide before infiltration with Spurr resin (TAAB Laboratories), and polymerized at 70 °C for 24 h. Infiltration times were increased to 48 h for *Drosophila* samples, to aid resin penetration through the abdominal cuticle. Ultrathin sections (70–90 nm) were prepared using a Reichert-Jung Ultracut E ultramicrotome, mounted on 150 mesh copper grids, contrast-stained using uranyl acetate and lead citrate, and examined on a FEI Tecnai 12 transmission microscope operated at 120 kV. Images were acquired with an AMT 16000 M digital camera. For stereological analysis (Howard and Reed 2010), 30 mitochondria from each group were aligned on a combined point counting grid composed of two sets of points of different densities on the same grid; nine fine points per coarse point. The volume of reference (mitochondria) was estimated as nine times the number of coarse points that cross the reference space. The volume of the particular phase (cristae) was estimated by counting the number of fine and coarse points that intersected the cristae.

Results

Transcription of Mitochondrial Respiratory Chain Genes

To determine whether oocyte mitochondria are transcriptionally active, we studied the expression of three mitochondrial genes, *nad1*, *cob*, and *cox1*. Each of these genes encodes a protein subunit of the respiratory electron transport chain, as shown schematically in figure 1*a*. mtDNA transcriptional rate has been correlated with energy output (Virbasius and Scarpulla 1994; Mehrabian et al. 2005). For *Drosophila* and zebrafish, we find that ovary has the lowest transcriptional rates for these three mitochondrial genes when compared with other somatic tissues and to sperm, as shown in figure 1*b*. In both species, we find that the quantity of the gene transcripts in ovary is approximately 15-fold lower than in active somatic tissues such as flight muscle in *Drosophila* and skeletal muscle in zebrafish. The difference between ovary and intestine was 3.2-fold for *Drosophila* and 5.5-fold for zebrafish (fig. 1*b*). We also detected normal levels of respiratory electron transport chain gene transcripts in testis, indicating that decreased mitochondrial transcription is specific to female gonads. qRT-PCR primers are as in supplementary table S1, Supplementary Material online, and statistical analysis of data is presented in supplementary table S2, Supplementary Material online.

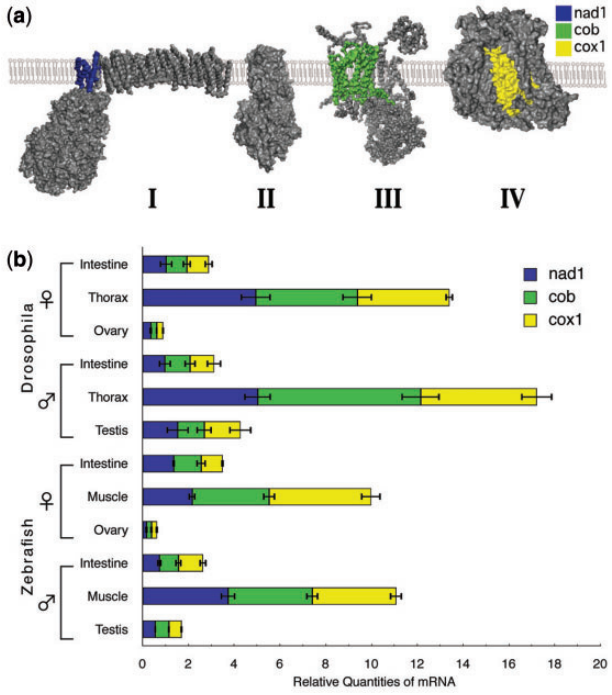

Fig. 1.—Relative quantities of mitochondrial mRNA measured for three key protein subunits of the mitochondrial respiratory chain. (*a*) A schematic representation of the respiratory electron transport chain of the mitochondrial inner membrane. The protein subunits highlighted in blue, green, and yellow represent the products of the mitochondrial genes *nad1*, *cob*, and *cox1*, respectively. Structures are surface models drawn using PyMol (Schrodinger 2010) from Protein Data Bank (PDB) atomic coordinate files with the following accession numbers: respiratory complex I (NADH-ubiquinone oxidoreductase), 3M9S; respiratory complex II (succinate dehydrogenase), 1ZOY; respiratory complex III (the cytochrome b-c_1 complex), 1QCR; complex IV (cytochrome *c* oxidase), 1V54. (*b*) Respiratory electron transport gene expression profile. Quantities are shown for mitochondrial mRNA expressed in different tissues of male and female individuals of *D. melanogaster* and *D. rerio*. The color coding is the same as that used in (*a*): blue, *nad1*; green, *cob*; yellow, *coxI*. Error bars indicate standard error of the mean (SEM). $P \leq 0.05$. See also supplementary tables S1 and S2, Supplementary Material online.

Mitochondrial Inner Membrane Potential

To further investigate the bioenergetic state of female germ line mitochondria, we performed confocal light microscopy using a combination of a mitochondrial marker with a proton motive force-reporting dye (Pendergrass et al. 2004). Mitochondria in *Drosophila* ovary at stages 5 and 7 (Bastock and St Johnston 2008) (fig. 2*a*) and zebrafish ovary at stages 3 and 4 (Selman et al. 1993) (fig. 2*b*) are seen to be in a quiescent state, with a decreased membrane potential compared

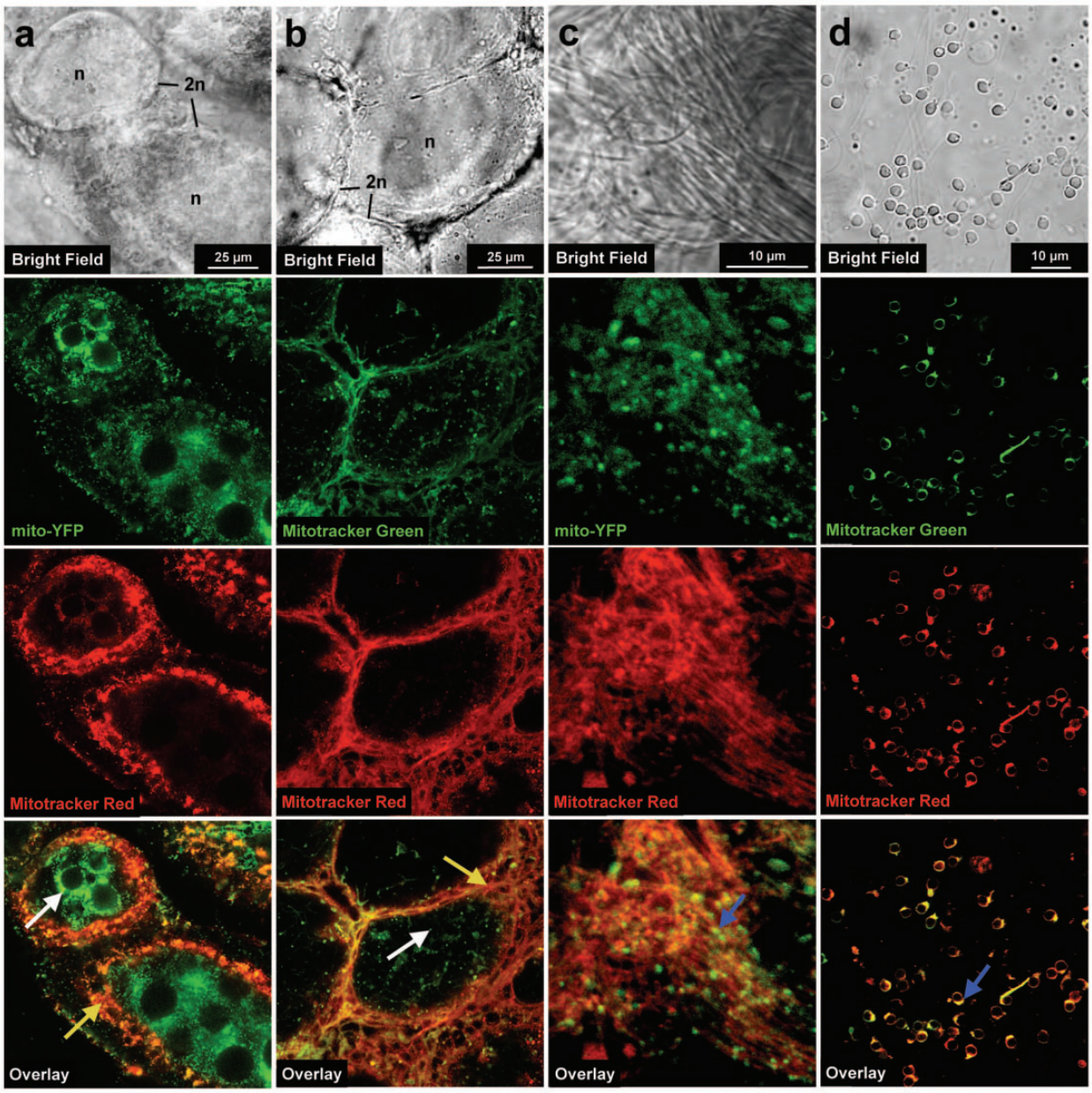

Fig. 2.—Mitochondrial inner membrane electrical potential visualized in ovary and sperm cells. Mitochondrial membrane potential in *Drosophila* ovary (*a*), zebrafish ovary (*b*), *Drosophila* sperm (*c*), and zebrafish sperm (*d*). The bright field micrograph shows the corresponding scale bars. Mitochondrial YFP (*Drosophila*) and Mitotracker Green FM (zebrafish) report the presence of intact mitochondria in the green channel. Mitotracker Red FM reports the relative membrane potential in those mitochondria in the red channel. Overlay of both channels highlights two different populations of mitochondria seen in (*a* and *b*) ovary. White arrows point to inactive female gamete mitochondria. Yellow arrows indicate somatic, active mitochondria, which accumulate the red dye indicating presence of membrane potential. In (*c*) and (*d*), blue arrows indicate active male gamete (sperm) mitochondria as a control. See also supplementary figure S1 and movie S1, Supplementary Material online.

with that in follicle cells. By contrast, sperm cells exhibit mitochondrial membrane potential typical of active ATP synthesis (*Drosophila*, fig. 2*c*; zebrafish, fig. 2*d*). There are clearly two broad classes of mitochondria in gonads—energy-transducing mitochondria of follicle, sperm, and somatic cells, and bioenergetically suppressed mitochondria in the ovary (fig. 2*a* and *b*). See also supplementary figure S1 and movie S1, Supplementary Material online.

Production of ROS

To estimate the production of ROS by female germ cells, *Drosophila* ovary at stages 3, 5, and 7 (fig. 3*a*), and zebrafish

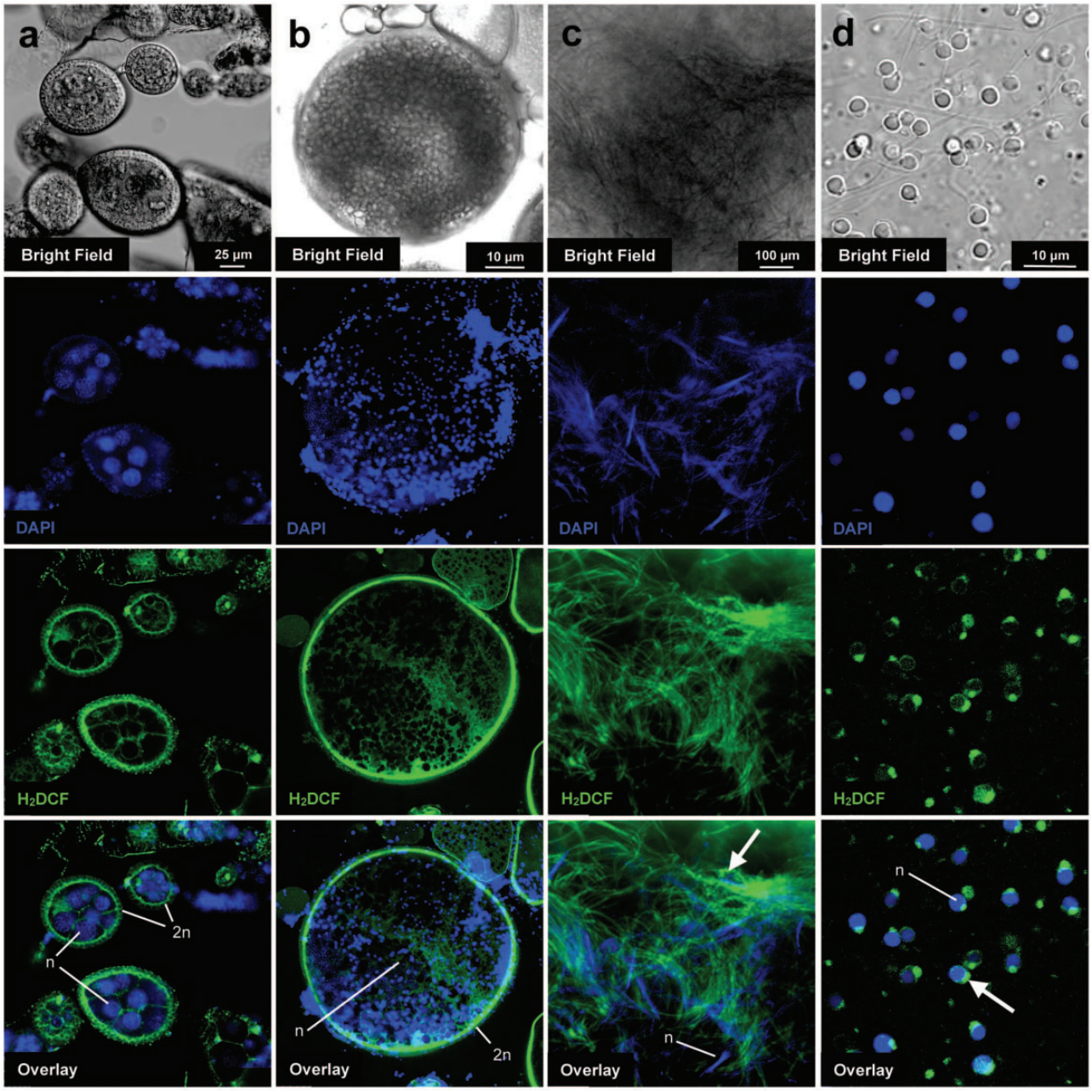

Fig. 3.—Mitochondrial production of ROS visualized in ovary and in sperm cells. ROS accumulation in *Drosophila* ovary (*a*), zebrafish ovary (*b*), *Drosophila* sperm (*c*), and zebrafish sperm (*d*). The bright field micrograph shows the corresponding scale bars. DAPI indicates nuclear DNA in the blue channel. Oxidized H_2DCF-DA is seen in the green channel and reports the relative amount of ROS in different tissues. Merged overlay of both channels highlights the abundance of ROS in diploid follicle cells compared with the female germ line cells in images (*a*) and (*b*), suggesting a reduced rate of electron transfer to oxygen in this cell type. Yellow arrows point to sperm mitochondria, which accumulate ROS as shown in images (*c*) and (*d*). See also supplementary figure S2 and movie S2, Supplementary Material online.

egg cell types I and II (fig. 3*b*) were stained with DAPI, visualizing DNA as blue, and with the ROS indicator H_2DCF-DA, which fluoresces green when oxidized. This fluorophore is used to estimate ROS production in situ (Owusu-Ansah et al. 2008). Within ovaries of *Drosophila* (fig. 3*a*) and zebrafish (fig. 3*b*), diploid follicle cells show, respectively, 50-fold and 100-fold higher H_2DCF-DA fluorescence intensity than the female germ cells that they surround (supplementary fig. S2, Supplementary Material online). We further certified that the differences in the fluorescence intensity found in those two cells types were not due to discrepancies in the number of mitochondria per cell and per area analyzed (supplementary

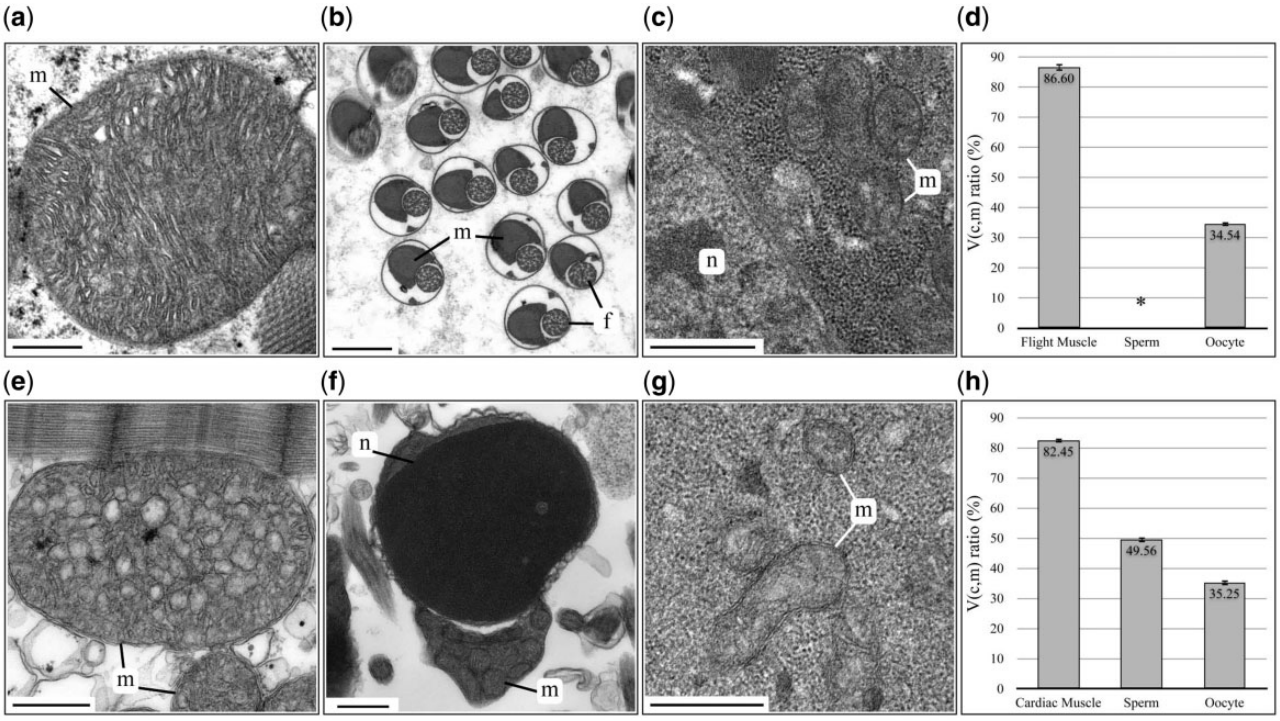

Fig. 4.—Mitochondrial ultrastructure in somatic cells and in male and female gametes. Transmission electron micrographs of *D. melanogaster* (*a*) flight muscle, (*b*) sperm, and (*c*) oocyte; and *D. rerio* (*e*) cardiac muscle, (*f*) sperm, and (*g*) oocyte. Letter (*m*) indicates mitochondria, (*n*) a haploid nucleus, and (*f*) a flagellum. Oocyte mitochondria are seen as simpler structures, ranging from 200 to 500 nm, lacking cristae development and matrix electron density (*c* and *g*). Muscle (*a* and *e*) and sperm (*b* and *f*) mitochondria were used as a somatic and male gametic tissue control samples for normal development, respectively. Images were taken using 9,300× magnification. The scale bar corresponds to 500 nm. Stereological analysis of the morphological variations among the three samples: (*d*) *Drosophila*; (*h*) *Danio*. *V*(*c*,*m*) is the ratio of crista volume to mitochondrion volume. Error bars are SEM, $P \leq 0.01$.

fig. S1, Supplementary Material online) but rather due to differences in mitochondrial activity. By contrast, sperm cells show H_2DCF-DA fluorescence in their mitochondria as seen in figure 3*c* for *Drosophila* and figure 3*d* for zebrafish. The results in figure 3 suggest that ROS production, like mtDNA transcription (fig. 1*b*), is repressed specifically in oocyte mitochondria. See also supplementary figure S2 and movie S2, Supplementary Material online.

Mitochondrial Ultrastructure

We examined the ultrastructural morphology of mitochondria in *Drosophila* flight muscle (fig. 4*a*) and zebrafish cardiac muscle (fig. 4*e*), in sperm (*Drosophila,* fig. 4*b*; zebrafish, fig. 4*f*), and in ovary (*Drosophila,* fig. 4*c*; zebrafish, fig. 4*g*). In fruitfly and zebrafish muscle (fig. 4*a* and *e*), the single mitochondrion in the field of view is large and has numerous cristae. It is also seen for both species that the mitochondrial matrix presents a relatively high density of the osmium stain. *Drosophila* sperm mitochondria (fig. 4*b*) are morphologically specialized, containing a paracrystalline lattice (Perotti 1973), and are therefore more difficult to compare. However, zebrafish sperm mitochondria (fig. 4*f*) show typical mitochondrial inner-membrane invagination and matrix density characteristic of metabolically active mitochondria. By contrast, *Drosophila* and zebrafish ovaries (fig. 4*c* and *g*, respectively), on the same scale, contain small (<0.5 μm) mitochondria of much simpler morphology, present in a cytoplasm rich in ribosomes and distinct from the nucleus from which it is separated by the characteristic nuclear double membrane (fig. 4*c*). In both species, stereological analysis confirms that oocyte mitochondrial cristae account for a much lower proportion of total mitochondrial volume than in other tissues (fig. 4*d* and *h* for *Drosophila* and zebrafish, respectively).

Discussion

Although errors in mtDNA replication have been demonstrated to produce inherited mitochondrial defects and aging in mice (Ross et al. 2013), animal mtDNA may also accumulate mutations in part because aerobic respiration generates mutagenic ROS in close proximity to mtDNA. Repair mechanisms, including base excision, may help to decrease or postpone pathological effects, while their failure to correct mtDNA mutation is implicated in, for example, human neurodegenerative disease (Santos et al. 2013). ROS-induced

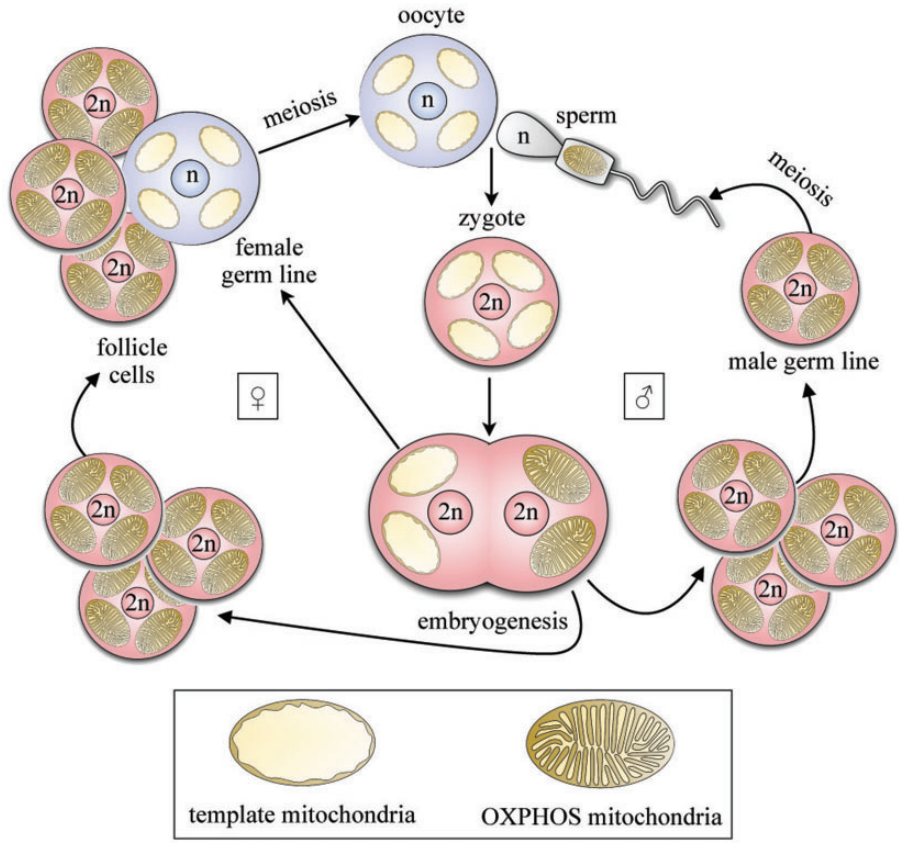

Fig. 5.—A model for maintenance of mtDNA by maternal inheritance of template mitochondria transmitted in the cytoplasm. An oocyte (egg cell) contains a nucleus with a haploid chromosome number (*n*) and a cytoplasm with multiple template mitochondria. A sperm cell, also with a haploid nucleus (*n*), is motile, and its motility requires ATP from active mitochondria performing oxidative phosphorylation (OXPHOS). Following fertilization, active sperm mitochondria are rapidly degraded, leaving only the maternal, template mitochondria in the cytoplasm of the diploid (*2 n*) zygote (or fertilized egg). Successive cell divisions in embryogenesis involve mitosis and differentiation—and division—of most template mitochondria into active OXPHOS mitochondria, which eventually dominate and populate not only somatic tissues but also the male germ line in which sperm are generated by meiosis in males for the next generation. However, some cells are sequestered and continue to carry only quiescent, template mitochondria, through meiosis and oogenesis to give the oocytes of females in the next generation. These cells comprise the female germ line. Female germ cells are never supplied with ATP by oxidative phosphorylation in their own mitochondria, but depend for their maintenance, at low metabolic rate, on ATP supplied, directly or indirectly, by neighboring somatic cells (follicle cells or nurse cells) that are specially adapted for this role. This hypothesis, after Allen (1996), predicts that the female germ line forms an indefinitely replicating vehicle for accurate transmission of mtDNA between generations. See also supplementary movie S3, Supplementary Material online.

mutation will be averted in the first place by repression of mitochondrial activity, giving decreased frequency of mutation, and a decrease in the rate of accumulation of mitochondrial mutational load. A further consequence of oocyte mitochondria acting as protected genetic templates is that full female fertility may depend upon absence of oocyte mitochondrial oxidative phosphorylation, rather than on its presence, as often supposed (Hsieh et al. 2004; Chappel 2013), whereas it is also clear that ATP synthesis proceeds in at least the majority of cells in the early mammalian embryo (Dumollard et al. 2007; Nunnari and Suomalainen 2012).

Repression of mtDNA transcription has been proposed as the evolutionary pressure that gave rise to the female germ line (Allen 1996). There is evidence for repressed respiratory oxygen uptake, complex IV activity, and ROS production in oocytes of the amphibian, *Xenopus laevis* (Kogo et al. 2011). Species lacking mtDNA or respiring anaerobically seem not to require a female germ line at all (Ayala 1998). Expression of mitochondrial and nuclear genes for individual respiratory chain complexes is coordinated, for example in mammalian neurons (Dhar et al. 2013), and repression of mtDNA transcription may be expected to result in effective silencing of corresponding nuclear genes for imported mitochondrial precursors.

The results presented here demonstrate that oocyte mitochondria are in a quiescent state in both a protostome (*D. melanogaster*) and a deuterostome (*D. rerio*), representing the two branches of the Bilateria. We interpret this result as a nonpathological condition that secures the faithful maternal transmission of mtDNA, from germ line to germ line, across

generations (Allen 1996). Even in exceptional species with doubly uniparental inheritance of mtDNA, only a female germ line gives rise to mitochondria of another female germ line, while the male germ line mitochondria can be inherited from either sex (Zouros et al. 1994; Ghiselli et al. 2013). It should be noted that uniparental inheritance of mitochondria is also the rule in single-celled eukaryotes, protists, with morphologically indistinguishable isogametes (Gyawali and Lin 2011). For multicellular eukaryotes, our conclusion is summarized in figure 5 and supplementary movie S3, Supplementary Material online. This interpretation is consistent with results reported for a cnidarian, the jellyfish *A. aurita* (de Paula et al. 2013), and might therefore be predicted to apply as a basic pattern of template mitochondrial transmission within the entire animal kingdom.

If quiescent, template mitochondria divide and differentiate into energetically active mitochondria, then the somatic cells and male gametes of each successive generation will be supplied with fresh mitochondria that are accurate copies of those previously supplied, furnishing cells with a supply of energy in the form of ATP for energy coupling in biosynthesis, transport, mechanical work, growth, and reproduction. Rather than envisaging a recovery of uncorrupted mtDNA from energetically active mitochondria, either by a genetic bottleneck (Samuels et al. 2010) or by purifying selection (Fan et al. 2008; Stewart et al. 2008), we suggest that the differentiation step from the genetic template is irreversible (Allen 1996). If this is correct, then a small subpopulation of template mitochondria will remain quiescent throughout animal development, and samples from this subpopulation will be transmitted indefinitely through successive female germ lines, eventually to populate both somatic and germ cells of each new generation (Allen and de Paula 2013)

It is possible that the evolutionary origin of separate sexes provided the solution to an inherent incompatibility between mitochondrial bioenergetic efficiency and fidelity of intergenerational transmission of mtDNA. Mitochondria are considered as key to the emergence of both eukaryotes (Martin and Muller 1998; Lane and Martin 2010) and multicellularity (Lane and Martin 2010; Blackstone 2013). Nevertheless, studies of the role of mitochondria in metazoan development tend to concentrate on direct metabolic and redox control of nuclear gene expression (Coffman 2009) rather than considering mitochondrial gene expression as an initiator or intermediary in orchestrated cell differentiation. It is also of interest to consider whether sexual dimorphism in gonad development (Mittwoch 2013) derives from dimorphism of mitochondria in the germ cells of the two sexes. In view of the complementarity of female and male mitochondria in a cnidarian (de Paula et al. 2013) as well as in examples of the two major branches of the Bilateria (this study), it seems likely that the requirement for a lineage of quiescent, genetic template mitochondria contributed to the evolutionary origin of the female germ line.

Supplementary Material

Supplementary figures S1 and S2, movies S1–S3, and tables S1 and S2 are available at *Genome Biology and Evolution* online (http://www.gbe.oxfordjournals.org/).

Acknowledgments

The authors thank K. Mandilaras and F. Combe for technical assistance, and C.A. Allen and I.M. Ibrahim for discussions. This work was supported by the Leverhulme Trust as research grant F/07 476/AQ to J.F.A., by the U.K. Natural Environment Research Council as research grant NE/G005516/1 to C.H.L., and by the Consejo Nacional de Ciencia y Tecnología Research Grant 179835 to F.M.

Literature Cited

Allen JF. 1996. Separate sexes and the mitochondrial theory of ageing. J Theor Biol. 180:135–140.
Allen JF, de Paula WBM. 2013. Mitochondrial genome function and maternal inheritance. Biochem Soc Trans. 41:1298–1304.
Ames BN, Shigenaga MK, Hagen TM. 1995. Mitochondrial decay in aging. Biochim Biophys Acta. 1271:165–170.
Anderson S, et al. 1981. Sequence and organization of the human mitochondrial genome. Nature 290:457–465.
Ayala FJ. 1998. Is sex better? Parasites say "no". Proc Natl Acad Sci U S A. 95:3346–3348.
Balaban RS, Nemoto S, Finkel T. 2005. Mitochondria, oxidants, and aging. Cell 120:483–495.
Bastock R, St Johnston D. 2008. *Drosophila* oogenesis. Curr Biol. 18: R1082–R1087.
Blackstone NW. 2013. Why did eukaryotes evolve only once? Genetic and energetic aspects of conflict and conflict mediation. Philos Trans R Soc B. 368:20120266.
Cao L, et al. 2009. New evidence confirms that the mitochondrial bottleneck is generated without reduction of mitochondrial DNA content in early primordial germ cells of mice. PLoS Genet. 5:e1000756.
Chappel S. 2013. The role of mitochondria from mature oocyte to viable blastocyst. Obstet Gynecol Int. 2013:183024.
Coffman JA. 2009. Mitochondria and metazoan epigenesis. Semin Cell Dev Biol. 20:321–329.
de Paula WBM, Lucas CH, Agip AN-A, Vizcay-Barrena G, Allen JF. 2013. Energy, ageing, fidelity and sex. Oocyte mitochondrial DNA as a protected genetic template. Philos Trans R Soc B. 368:20120263.
Dhar SS, Johar K, Wong-Riley MTT. 2013. Bigenomic transcriptional regulation of all thirteen cytochrome c oxidase subunit genes by specificity protein 1. Open Biol. 3:120176.
Dumollard Rm, Duchen M, Carroll J. 2007. The role of mitochondrial function in the oocyte and embryo. In: Justin CSJ, editor. Current topics in developmental biology. Waltham (MA): Academic Press. p. 21–49.
Fan W, et al. 2008. A mouse model of mitochondrial disease reveals germline selection against severe mtDNA mutations. Science 319: 958–962.
Ghiselli F, et al. 2013. Structure, transcription, and variability of metazoan mitochondrial genome: perspectives from an unusual mitochondrial inheritance system. Genome Biol Evol. 5:1535–1554.
Gray MW, Burger G, Lang BF. 1999. Mitochondrial evolution. Science 283: 1476–1481.
Gyawali R, Lin X. 2011. Mechanisms of uniparental mitochondrial DNA inheritance in *Cryptococcus neoformans*. Mycobiology 39: 235–242.

Harman D. 1972. The biologic clock: the mitochondria? J Am Geriatr Soc 20:145–147.
Howard CV, Reed MG. 2010. Unbiased stereology: three-dimensional measurement in microscopy, Liverpool (United Kingdom): QTP Publications.
Hsieh RH, et al. 2004. Decreased expression of mitochondrial genes in human unfertilized oocytes and arrested embryos. Fertil Steril. 81(suppl 1), 912–918.
Jenuth JP, Peterson AC, Fu K, Shoubridge EA. 1996. Random genetic drift in the female germline explains the rapid segregation of mammalian mitochondrial DNA. Nat Genet. 14:146–151.
Kogo N, et al. 2011. Germ-line mitochondria exhibit suppressed respiratory activity to support their accurate transmission to the next generation. Dev Biol. 349:462–469.
LaJeunesse DR, et al. 2004. Three new *Drosophila* markers of intracellular membranes. BioTechniques 36:784–788, 790.
Lane N, Martin W. 2010. The energetics of genome complexity. Nature 467:929–934.
Lill R, Kispal G. 2000. Maturation of cellular Fe-S proteins: an essential function of mitochondria. Trends Biochem Sci. 25:352–356.
Martin W, Muller M. 1998. The hydrogen hypothesis for the first eukaryote. Nature 392:37–41.
Mehrabian Z, Liu LI, Fiskum G, Rapoport SI, Chandrasekaran K. 2005. Regulation of mitochondrial gene expression by energy demand in neural cells. J Neurochem 93:850–860.
Mitchell P. 1961. Coupling of phosphorylation to electron and hydrogen transfer by a chemi-osmotic type of mechanism. Nature 191:144–148.
Mittwoch U. 2013. Sex determination. Embo Rep. 14:588–592.
Nunnari J, Suomalainen A. 2012. Mitochondria: in sickness and in health. Cell 148:1145–1159.
Owusu-Ansah E, Yavari A, Banerjee U. 2008. A protocol for in vivo detection of reactive oxygen species. Protoc Exchange. Advance Access published February 27, 2008, doi:10.1038/nprot.2008.23.
Pendergrass W, Wolf N, Poot M. 2004. Efficacy of MitoTracker Green and CMXrosamine to measure changes in mitochondrial membrane potentials in living cells and tissues. Cytometry A. 61:162–169.
Perotti ME. 1973. The mitochondrial derivative of the spermatozoon of *Drosophila* before and after fertilization. J Ultrastruct Res. 44:181–198.
Pesole G, et al. 2012. The neglected genome. Embo Rep. 13:473–474.
Ross JM, et al. 2013. Germline mitochondrial DNA mutations aggravate ageing and can impair brain development. Nature 501:412–415.
Sadraie M, Missirlis F. 2011. Evidence for evolutionary constraints in *Drosophila* metal biology. Biometals 24:679–686.
Samuels DC, Wonnapinij P, Cree LM, Chinnery PF. 2010. Reassessing evidence for a postnatal mitochondrial genetic bottleneck. Nat Genet. 42:471–472; author reply 472–473.
Santos RX, et al. 2013. Mitochondrial DNA oxidative damage and repair in aging and Alzheimer's disease. Antioxid Redox Signal. 18: 2444–2457.
Schneider CA, Rasband WS, Eliceiri KW. 2012. NIH Image to ImageJ: 25 years of image analysis. Nat Methods. 9:671–675.
Schrodinger L, 2010. The PyMOL molecular graphics system Version 1.3r1. Schrödinger, LLC.
Selman K, Wallace RA, Sarka A, Qi X. 1993. Stages of oocyte development in the zebrafish *Brachydanio rerio*. J Morphol. 218:203–224.
Stewart JB, et al. 2008. Strong purifying selection in transmission of mammalian mitochondrial DNA. PLoS Biol. 6:e10.
Vaux DL, Cory S, Adams JM. 1988. Bcl-2 gene promotes haemopoietic cell survival and cooperates with c-myc to immortalize pre-B cells. Nature 335:440–442.
Virbasius JV, Scarpulla RC. 1994. Activation of the human mitochondrial transcription factor A gene by nuclear respiratory factors: a potential regulatory link between nuclear and mitochondrial gene expression in organelle biogenesis. Proc Natl Acad Sci U S A. 91:1309–1313.
Wai T, Teoli D, Shoubridge EA. 2008. The mitochondrial DNA genetic bottleneck results from replication of a subpopulation of genomes. Nat Genet. 40:1484–1488.
Wallace DC. 2007. Why do we still have a maternally inherited mitochondrial DNA? Insights from evolutionary medicine. Annu Rev Biochem. 76:781–821.
Wallace DC. 2010. Mitochondrial DNA mutations in disease and aging. Environ Mol Mutagen. 51:440–450.
Wallace DC, et al. 1995. Mitochondrial DNA mutations in human degenerative diseases and aging. Biochim Biophys Acta. 1271:141–151.
Zimprich F, Ashworth R, Bolsover S. 1998. Real-time measurements of calcium dynamics in neurons developing in situ within zebrafish embryos. Pflugers Archiv. 436:489–493.
Zouros E, Ball AO, Saavedra C, Freeman KR. 1994. An unusual type of mitochondrial-DNA inheritance in the blue mussel *Mytilus*. Proc Natl Acad Sci U S A. 91:7463–7467.

Associate editor: Bill Martin